

DOI: 10.1002/cctc.201300550



Type II Flavin-Containing Monooxygenases: A New Class of Biocatalysts that Harbors Baeyer–Villiger Monooxygenases with a Relaxed Coenzyme Specificity

Anette Riebel,^[a] Michael J. Fink,^[b] Marko D. Mihovilovic,^[b] and Marco W. Fraaije*^[a]

Within a newly identified set of flavin-containing monooxygenases (FMOs) from *Rhodococcus jostii* RHA1, we have identified three monooxygenases (FMO-E, FMO-F, and FMO-G) that are effective in catalyzing Baeyer–Villiger oxidations. These type II FMOs display relaxed coenzyme specificity by accepting both NADPH (reduced form of nicotinamide adenine dinucleotide phosphate) and NADH (reduced form of nicotinamide adenine dinucleotide), as a coenzyme, which is a novel and attractive feature among biocatalysts capable of conducting Baeyer–Villiger oxidations. We purified FMO-E and determined that the Michaelis constants for both coenzymes were in the micromolar range, whereas the activity was highest for NADH. By using the stopped-flow technique, formation of a peroxyflavin-enzyme intermediate was observed, which indicated that

type II FMOs follow a catalytic mechanism similar to that of other class B flavoprotein monooxygenases. A set of cyclobutanones and cyclohexanones were used to probe the regio- and enantioselectivity of all three recombinant monooxygenases. The biocatalysts readily accepted small cyclic ketones, which enabled the conversion of previously poorly accepted substrates by other monooxygenases (especially norcamphor), and exhibited excellent and unique regio- and enantioselectivities. Sequence analysis revealed that type II FMOs that act as Baeyer–Villiger monooxygenases contain a unique N-terminal domain. Sequence conservation in this protein domain can be used to identify new NADH-dependent Baeyer–Villiger monooxygenases, which would facilitate future biocatalyst discovery efforts.

Introduction

Flavoprotein monooxygenases (MOs) represent potent catalytic tools for the production of high-value chemical building blocks and pharmaceuticals.^[1] These oxygenating biocatalysts are able to perform efficient chemo-, regio-, and/or enantioselective oxygenation reactions by using only dioxygen and reducing equivalents such as NADH [reduced form of nicotinamide adenine dinucleotide (NAD⁺)] and NADPH [reduced form of nicotinamide adenine dinucleotide phosphate (NADP⁺)].^[2] Flavoprotein MOs can be classified into six structurally and mechanistically distinct classes (Figure 1). Upon taking into account the differences in structural and mechanistic properties of the various flavoprotein MO classes, class A and B monooxygenases are especially interesting for biocatalysis, as they are single-component enzymes with a typically tightly bound flavin adenine dinucleotide (FAD) cofactor.

Class A flavoprotein MOs have been shown to be specialized in hydroxylation and epoxidation reactions.^[2] Class B typically

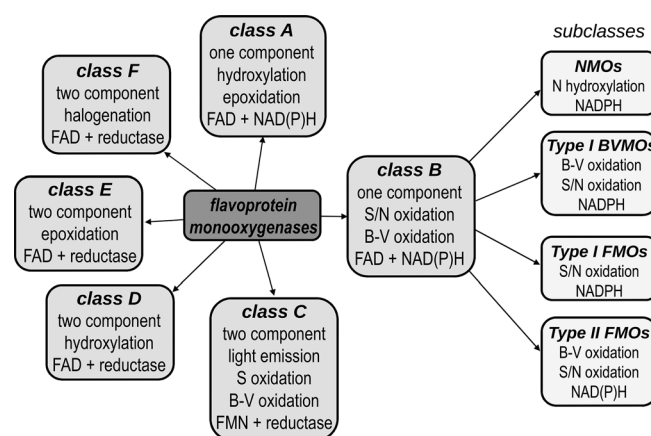


Figure 1. Overview of the different flavoprotein monooxygenase classes; B-V oxidation = Baeyer–Villiger oxidations, FMN = flavin mononucleotide.

covers Baeyer–Villiger and heteroatom oxidations.^[2] Careful analysis of the sequence and enzymatic properties of the latter class has revealed several distinct subclasses (Figure 1). An extensively studied subclass is formed by type I Baeyer–Villiger monooxygenases (BVMOs): these carbonyl- and heteroatom-oxidizing enzymes are specific towards NADPH as a cofactor.^[3] Three other subclasses of class B flavoprotein MOs are known to date. Type I flavin-containing monooxygenases (FMOs), also NADPH dependent, have mainly been studied for their role in human metabolism.^[4] The human proteome contains six type I

[a] A. Riebel, Prof. Dr. M. W. Fraaije
Molecular Enzymology group
University of Groningen
Nijenborgh 4, 9747 AG Groningen (The Netherlands)
Fax: (+31) 503634165
E-mail: m.w.fraaije@rug.nl

[b] Dr. M. J. Fink, Prof. Dr. M. D. Mihovilovic
Institute of Applied Synthetic Chemistry
Vienna University of Technology
Getreidemarkt 9/163-OC, 1060 Vienna (Austria)

Supporting information for this article is available on the WWW under <http://dx.doi.org/10.1002/cctc.201300550>.

FMO isoforms, all of which have been reported as important in the oxidative degradation of nitrogen- and sulfur-containing compounds. Only recently, some microbial representatives were discovered and shown to represent interesting biocatalysts for oxidizing secondary amines, including the conversion of indole into indigo blue.^[5] Another class B subclass contains microbial MOs that hydroxylate primary amines, for example, lysine N6-hydroxylase and ornithine N5-hydroxylase. In reference to their reactivity, these are named N-hydroxylating MOs (NMOs). All together, these biocatalyst subclasses share a pronounced preference towards NADPH as a cofactor.

Recently, we identified a new group of sequence-related enzymes that belong to class B flavoprotein MOs: type II FMOs (Figure 1). We reported on seven type II FMOs derived from the genome of *Rhodococcus jostii* RHA1.^[6] Their unique sequence profiles as well as their relaxed coenzyme specificity legitimated a classification separate from the other class B flavoprotein MOs, together with an already previously discovered MO of *Stenotrophomonas maltophilia*.^[7] Within these seven newly found type II FMOs, however, we found significant differences concerning substrate acceptance. FMO-E, FMO-F, and FMO-G efficiently catalyzed Baeyer–Villiger oxidation of two ketones [i.e., bicyclo[3.2.0]hept-2-en-6-one (1) and phenylacetone (3)], a catalytic feature that was so far only known for type I BVMOs. However, in marked contrast to type I BVMOs, all type II FMOs were shown to be able to use NADPH or NADH indifferently. This seems particularly interesting for combining such enzymes with other redox biocatalysts in multistep biotransformation cascades and thus encouraged us to perform an in-depth study of the newly identified type II FMOs that can act as bona fide BVMOs.

Results and Discussion

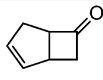
Within this work, mechanistic, kinetic, and structural aspects of type II FMO-catalyzed Baeyer–Villiger oxidations were investigated by using FMO-E as a model enzyme. Biocatalytic performance was then assessed for all three biocatalysts.

Purification of FMO-E

To allow efficient one-step purification, we produced FMO-E, FMO-F, and FMO-G with an N-terminal strep-tag (in pBADNS). Purification trials revealed that only FMO-E could be isolated in good yields. The other MOs were found to suffer from FAD loss during the purification procedure. As all three biocatalysts are sequence related, we decided to use FMO-E as a prototype for biochemical characterization. From a 1 L culture, 25 mg of pure FMO-E could be obtained. The purified enzyme displays a typical flavin absorbance spectrum, with characteristic maxima at 451 and 381 nm. The extinction coefficient was determined as $11.9 \text{ mM}^{-1} \text{ cm}^{-1}$ ($\epsilon_{451 \text{ nm}}$). Furthermore, from the measured absorbance ratio $A_{280}/A_{451} = 10$, it was concluded that the protein was purified as a holoenzyme.

Kinetic characterization of FMO-E

Using purified FMO-E, steady-state kinetic parameters were determined for ketone 1, NADH, and NADPH (Table 1). For both coenzymes and the ketone, typical Michaelis–Menten behavior was observed, which yielded the catalytic (k_{cat}) and Michaelis

Substrate/coenzyme	K_M [mM]	k_{cat} [s^{-1}]
bicyclo[3.2.0]hept-2-en-6-one (1): 	19.8	2.7
NADPH	< 0.0010	2.7
NADH	0.0054	4.3

constants (K_M). Even though FMO-E accepts both nicotinamide coenzymes, the enzyme appears to have a higher affinity (K_M) for NADPH. Yet, the value of K_M for NADH is also in the low micromolar range, and k_{cat} for NADH is higher than that for NADPH (4.3 vs. 2.7 s^{-1}). This indicates that FMO-E is an efficient enzyme with NADH as the coenzyme, which is in contrast to most other class B flavoprotein MOs. Also, all other type II FMOs have shown coenzyme indifference.^[6] The determined k_{cat} values also confirm that FMO-E is a potent biocatalyst, as the rate of catalysis is in the same range as that found for other class B flavoprotein MOs (k_{cat} values for type I BVMOs phenylacetone MO^[8] and cyclohexanone MO^[9] are typically in the range of $1\text{--}20 \text{ s}^{-1}$). It is particularly noteworthy that the k_{cat} values determined for type II FMO from *S. maltophilia*^[7] are two orders of magnitude lower (0.029 s^{-1}), and this makes the title enzyme a more likely candidate for biocatalytic processes. Interestingly, for both bacterial monooxygenases the rate of catalysis was highest if NADH was used. This may hint to a role of the coenzyme in the rate-limiting step of the kinetic mechanism of this MO. For type I BVMO cyclohexanone MO, it has been shown that NADP^+ release limits the rate of catalysis.^[9]

To establish whether FMO-E follows a catalytic mechanism similar to that of type I FMOs and type I BVMOs, stopped-flow experiments were performed. The kinetic mechanism of flavoprotein MOs can be subdivided into reductive and oxidative half-reactions. Reduction of the FAD cofactor by the nicotinamide coenzyme is considered as the reductive half-reaction. Anaerobic reduction of FMO-E by NADPH was monitored over time by using a stopped-flow instrument, which revealed a relatively high rate of reduction (17.5 s^{-1}) at a saturating NADPH concentration.

In the next step, the reduced flavin of class B flavoprotein MOs is able to swiftly react with molecular oxygen typically to yield a relatively stable peroxyflavin intermediate. The ability to stabilize such a reactive enzyme intermediate in the absence of a substrate has been the typical hallmark of this biocatalyst class. For monitoring the above-described oxidative half-reaction, NADPH-reduced FMO-E was rapidly mixed with aerated buffer. Analysis of the obtained spectra revealed that the data

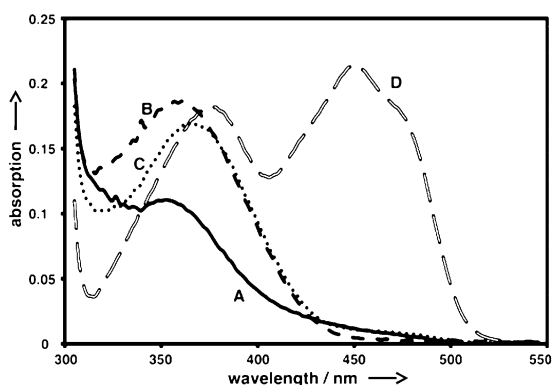


Figure 2. Deconvoluted flavin absorbance spectra upon mixing FMO-E with air-saturated buffer. The spectra were reconstructed by using the model $A \rightarrow B \rightarrow C \rightarrow D$ with rates of 7.2, 1.2, and 0.5 s^{-1} , respectively. A) Reduced state, B) first peroxyflavin intermediate, C) second peroxyflavin intermediate, D) oxidized state.

could be best fitted with an irreversible three-step model ($A \rightarrow B \rightarrow C \rightarrow D$, Figure 2). Directly after mixing with oxygen, species B is rapidly formed with a rate of 7.2 s^{-1} , as evidenced by an absorbance band at approximately 365 nm. This perfectly matches the spectral features of a peroxyflavin intermediate and confirms that FMO-E operates through a catalytic mechanism similar to that of other class B flavoprotein MOs. This intermediate (spectrum B) undergoes slow and modest spectral change (1.2 s^{-1}) to form a less-intense absorbance band (spectrum C). This transition may represent a change in the protonation state of the peroxyflavin or a conformational change and has also been observed for type I BVMOs.^[10,11] In a subsequent slow process (0.5 s^{-1}), the flavin is oxidized (spectrum D), which is accompanied by the formation of hydrogen peroxide. These kinetic and spectral properties closely resemble the kinetic behavior of other class B flavoprotein MOs.

Structural analysis of FMO-E

To obtain a better view on how FMO-E is able to catalyze Baeyer–Villiger oxidations, we compared a structural model of FMO-E with the crystal structures of a type I BVMO (i.e., PDB 1W4X)^[12] and a type I FMO (i.e., PDB 2VQ7).^[13] Comparison of the active sites clearly showed that all three enzymes employ different strategies to catalyze such oxygenations (Figure 3).

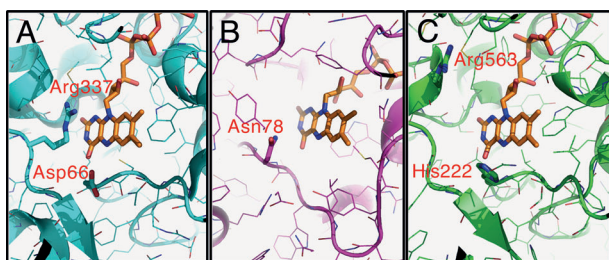


Figure 3. Comparison of the active site architectures of a) PDB:1W4X as a type I BVMO, b) 2VQ7 as a type I FMO, and c) FMO-E as the type II FMO.

In type I BVMOs, a strictly conserved arginine is crucial for catalysis; in type I FMOs, an asparagine residue serves such a role, but in the model of FMO-E no such active residue was identified in the homologous structural positions. Yet, a histidine and an arginine residue were found to be positioned close to the isoalloxazine moiety of the FAD cofactor, possibly assisting in catalysis. Both residues are conserved among type II FMO sequences. Unfortunately, the protein sequences of FMO-E and the type II FMO from *S. maltophilia*^[7] are too dissimilar to locate the mutated residues in the structure of the latter monooxygenase. To verify whether His222 and Arg563 serve a role in catalysis, the corresponding alanine mutants were prepared. The first evidence of changed catalytic capacities of the mutants could directly be seen upon growing cultures under optimal expression conditions. For wild-type FMO-E, it was observed that the color of the growth medium changed significantly. This was due to the formation of a blue pigment that was formed upon oxidative conversion of indigenous indole into indigo blue.^[6] Expression of the mutants did not result in any color change in the medium. Furthermore, purification of the mutant enzymes resulted in only inactive apoprotein, and the addition of FAD to the apoprotein samples did not restore any activity. Tests with cleared cell extracts containing the different mutant enzymes showed that the activity was affected dramatically: conversion of thioanisole (**2**) dropped from 56%^[6] to only 6%, whereas phenylacetone (**3**) and bicyclo[3.2.0]heptenone (**1**) were not converted at all under the standard assay conditions. These results show that the targeted residues are essential for proper FAD binding and, furthermore, provide no conclusive evidence on whether the residues are important for catalysis.

Intriguingly, on the protein sequence level, the type II FMOs described in this paper all share an extra N-terminal extension of approximately 160 residues in comparison with the other four rhodococcal type II FMOs and the type II FMO from *S. maltophilia*. This aberrant sequence feature coincides with the potency to efficiently catalyze Baeyer–Villiger oxidations. The molecular basis for this correlation is unclear. However, it may be used to identify new type II FMOs that can be exploited as NADH-driven biocatalysts for Baeyer–Villiger oxidations. A BLASTP search by using the N-terminal sequence of FMO-E (170 residues) resulted in the identification of 545 type II FMOs containing the typical N-terminal extension. All these hits displayed >25% sequence identity in the N terminus, and they also contain the typical GxGxxG Rossmann fold motifs in the C-terminal region, which confirmed that they are FAD-containing NAD(P)H-dependent monooxygenases. These putative MOs are mainly found in fungal genomes and none of them has been explored as a biocatalyst so far.

Biocatalytic exploration

As type II FMOs are fundamentally different from type I BVMOs, we set out to explore the substrate acceptance range and stereoselective properties of all three FMOs studied as whole-cell biocatalysts. For this, 14 ketones [6 prochiral cyclobutanones **4–9**, 4 prochiral cyclohexanones **10–13**, 3 racemic

fused cyclobutanones **1**, **14**, **15**, and racemic norcamphor (**16**) were tested as substrates (see Tables 2 and 3 for their structural formulas).

Desymmetrization of prochiral cyclobutanones and cyclohexanones revealed a clear preference (Table 2). All three monooxygenases efficiently converted most cyclobutanones, whereas the cyclohexanones were poorly accepted as substrates or not at all. The corresponding lactones were formed with moderate to good enantioselectivity (from 5 to 79% *ee*, median 45% *ee*). Interestingly, type II FMOs displayed complementary enantio-

preference in all cases, which enabled the synthesis of both optical antipodes in enantioenriched form.

Motivated by the good results from prochiral cyclobutanone transformations, we decided to test the performance of these new Baeyer–Villiger catalysts in another reaction mode: regio-divergent conversion of racemic fused cycloketones **1** and **14**–**16**. Gratifyingly, the MOs were capable of converting all four tested ketones (Table 3), which resulted in preferential formation of normal lactones (in this case, the rearrangement was governed by higher nucleophilicity, that is, a higher degree of

substitution of the migrating carbon atom). This kind of regioselectivity is known from type I BVMOs of the cyclopentanone monooxygenase cluster.^[15] Most interestingly, the title FMOs are the only Baeyer–Villiger biocatalysts known to be able to perform kinetic resolution of norcamphor (**16**) to the normal lactone with both excellent stereoselectivity and yield. The best reported enzyme for this transformation, type I BVMO cyclododecanone MO from *Rhodococcus ruber* SC1,^[16] catalyzes the formation of both regioisomers of norcamphor with excellent enantioselectivity (>98%), but in almost equimolar ratio (57:43 normal/abnormal) and at a rather low rate. Specifically, FMO-F and FMO-G display excellent enantioselectivities ($E > 200$) and regioselectivities (>99:1 for

Table 2. Desymmetrization of cyclobutanones and cyclohexanones by FMO-E, FMO-F, and FMO-G by using whole cells.^[a]

Compound	Substrate structure	R	FMO-E		FMO-F		FMO-G	
			Rel. conv. [%]	<i>ee</i> [%]	Rel. conv. [%]	<i>ee</i> [%]	Rel. conv. [%]	<i>ee</i> [%]
4		Bn	>99	16 (S)	90	40 (R)	95	50 (R)
5		Ph	>99	69 (R)	96	78 (S)	93	67 (S)
6		<i>p</i> C ₆ H ₄	>99	79 (R)	76	64 (S)	67	47 (S)
7		<i>p</i> MeOC ₆ H ₄ CH ₂	98	5 (S)	75	18 (S)	99	42 (R)
8		3,4-OCH ₂ O-C ₆ H ₃ CH ₂	73	30 (R)	83	50 (S)	40	40 (S)
9		3,4,5-(MeO) ₃ C ₆ H ₂ CH ₂	10	13 (R)	n.c.	n.a.	n.c.	n.a.
10		Me	n.c.	n.a.	n.c.	n.a.	n.c.	n.a.
11		CO ₂ Et	12	99 (+) ^[b]	n.c.	n.a.	n.c.	n.a.
12		Ph	n.c.	n.a.	n.c.	n.a.	n.c.	n.a.
13			n.c.	n.a.	n.c.	n.a.	n.c.	n.a.

[a] The relative conversion (Rel. conv.) and *ee* values of the lactone products were determined by chiral-phase GC-FID after a biotransformation time of 24 h. The absolute configuration or sign of the optical rotation of the lactone products was assigned on the basis of published reference biotransformations.^[14] n.a. = Not applicable, n.c. = no conversion. [b] Absolute configuration of the product is not known; the sign of the optical rotation is given instead.

Table 3. Regiodivergent oxidation of racemic fused cyclobutanones *rac*-**1**, **14**, **15** and norcamphor (*rac*-**16**) by FMO-E, FMO-F, and FMO-G by using whole cells.^[a]

Compound	Substrate structure	FMO-E			FMO-F			FMO-G		
		Rel. conv. [%] N/ABN	<i>ee</i> _N [%] <i>ee</i> _{ABN} [%]	<i>E</i> _N <i>E</i> _{ABN}	Rel. conv. [%] N/ABN	<i>ee</i> _N [%] <i>ee</i> _{ABN} [%]	<i>E</i> _N <i>E</i> _{ABN}	Rel. conv. [%] N/ABN	<i>ee</i> _N [%] <i>ee</i> _{ABN} [%]	<i>E</i> _N <i>E</i> _{ABN}
1		97 14:86	46 (3 <i>aR</i> ,6 <i>aS</i>) 3 (3 <i>aR</i> ,6 <i>aS</i>)	n.d. n.d.	92 12:88	19 (3 <i>aS</i> ,6 <i>aR</i>) 6 (3 <i>aR</i> ,6 <i>aS</i>)	n.d. n.d.	81 20:80	21 (3 <i>aS</i> ,6 <i>aR</i>) <i>rac</i>	n.d. n.d.
14		81 95:5	39 (3 <i>aS</i> ,7 <i>aS</i>) 98 (3 <i>aR</i> ,7 <i>aS</i>)	n.d. n.d.	77 92:8	44 (3 <i>aS</i> ,7 <i>aS</i>) 71 (3 <i>aR</i> ,7 <i>aS</i>)	137 59	91 92:8	18 (3 <i>aS</i> ,7 <i>aS</i>) 75 (3 <i>aR</i> ,7 <i>aS</i>)	n.d. n.d.
15		>99 >99:1	<i>rac</i> n.a.	n.d. n.a.	77 >99:1	91 ^[b] n.d.	99 n.d.	99 >99:1	<i>rac</i> n.a.	n.d. n.a.
16		14 >99:1	94 (1 <i>S</i> ,5 <i>R</i>) n.a.	36 n.a.	22 >99:1	>99 (1 <i>S</i> ,5 <i>R</i>) n.a.	>200 n.a.	47 99:1	99 (1 <i>S</i> ,5 <i>R</i>) n.d.	>200 n.a.

[a] The relative conversion (Rel. conv.) and *ee* values of the lactone products were determined by chiral-phase GC-FID after a biotransformation time of 24 h. Selectivity values *E* in kinetic resolution-type reactions were calculated according to Sih's equation: $E = [\ln(1 - ee_s) - \ln(1 + ee_s/ee_p)] / [\ln(1 + ee_s) - \ln(1 + ee_s/ee_p)]$, in which *S* = substrate and *P* = product. N = normal lactones, ABN = abnormal lactones are given in italics. Absolute configuration or sign of the optical rotation of the lactone products was assigned on the basis of published reference biotransformations.^[15] n.a. = Not applicable, n.d. = not determined, *rac* = racemic. [b] Product regioisomers were not separable by preparative low-pressure chromatography; for assignment of the regio- and stereoisomers, see Ref. [15].

normal/abnormal lactone) for the oxygenation of this natural compound.

Clearly, the studied type II FMOs display biocatalytic features that set them apart from type I BVMOs. Although the enantioselectivity is far from pharmaceutical standards in many cases and higher substrate titers were not investigated within this project, these enzymes nevertheless represent a new and promising group of oxidative biocatalysts.

Conclusions

Within the newly described class of type II FMOs, we identified three FMOs that could efficiently catalyze Baeyer–Villiger oxidations. The exemplary kinetic analysis of FMO-E revealed that it is catalytically competent by displaying high affinities towards both nicotinamide coenzymes NADH and NADPH with significantly higher catalytic rates than that of a recently reported type II FMO from *S. maltophilia*. The pre-steady-state kinetic analysis of FMO-E revealed a catalytic mechanism that was similar to that of other class B MOs:

- 1) Oxidized FMO-E is rapidly reduced by a reduced coenzyme without the need for substrate binding.
- 2) The reduced FMO-E rapidly reacts with molecular oxygen.
- 3) FMO-E is able to form a stable peroxyflavin intermediate.

For all other studied class B monooxygenases, it was shown that the oxidized nicotinamide coenzyme remained bound to the active site until the peroxyflavin had oxygenated the substrate. Only then was it released, often in a relatively slow kinetic event. Such a scenario fits with the steady-state and pre-steady-state kinetic data of FMO-E in which $\text{NADP}^+/\text{NAD}^+$ was released in a relatively slow process. More detailed kinetic and structural studies will settle this issue.

A major disadvantage of the well-studied type I BVMOs is their high specificity for NADPH, a relatively expensive cofactor in comparison to NADH. Moreover, attempts to engineer a NADH-accepting type I BVMO have so far not been successful.^[17,18] Given that the studied FMO-E, FMO-F, and FMO-G enzymes can act as BVMOs with NADH as the coenzyme, they represent highly sought-after biocatalysts. This way, a significantly better balanced exploitation of the available reduction equivalents within a metabolically active cell may be achieved, which would alleviate the metabolic burden of such systems. Additionally, higher compatibility and flexibility may be achieved upon designing redox cascades in a cell-free environment.

This study showed that the tested type II FMOs could indeed be used as efficient biocatalysts. By testing a set of small cycloketones we unveiled new and excellent stereoselectivities; for example, the conversion of norcamphor (**16**) by FMO-F proceeds with > 99% regioselectivity and > 99% enantioselectivity. Such selectivity has not been observed before with previously identified BVMOs. This may be explained by the fact that type II FMOs are only distantly related to type I BVMOs. As a consequence, they will exhibit totally different active-site architectures. In fact, FMOs seem to lack the typical

catalytic residues that are employed in type I BVMOs and type I FMOs. By site-directed mutagenesis, we determined that His222 and Arg563 are crucial for the functioning of FMO-E. Elucidation of the structure of FMO-E would shed light on the structural and catalytic properties of this NAD(P)H-dependent monooxygenase. At this point, the striking discovery of the N-terminal extension in Baeyer–Villiger active FMOs can serve as a search template in biocatalytically uncharted space: many more type II FMOs await exploration and future research will reveal how they operate at the molecular level.

Experimental Section

Reagents and enzymes

Oligonucleotide primers were purchased from Sigma, dNTPs and the In-Fusion 2.0 CF Dry-Down PCR Cloning Kit were purchased from Clontech, and Phusion polymerase was purchased from Finnzymes. All other chemicals were obtained from Acros Organics, ABCR, Sigma–Aldrich, TCI Europe, and Roche Diagnostics GmbH.

Bacterial strains and Plasmids

Escherichia coli TOP10 from Invitrogen was used as a host for DNA manipulations and protein expression. The used expression vector was a modified pBAD vector (pBADN) in which the *Nde*I site was replaced by the original *Nco*I site.^[19] For this study, we introduced a strep-tag binding site (TGG AGC CAC CCG CAG TTT GAA AAA) followed by a TEV protease cleavage site (GAG AAT TTA TAT TTT CAA GGT) between the promoter and the start codon of the gene to be cloned to yield the pBADNS vector.

Sequence analysis, cloning, expression, and protein purification

The NCBI server (blast.ncbi.nlm.nih.gov/Blast.cgi) was used for DNA sequence retrieval and BLAST searches. The EBI server (www.ebi.ac.uk/Tools/msa/clustalw2/) was used for multiple sequence alignment by CLUSTALW.^[19] The FMO-E sequence was used as input to prepare a structural model by using the CPH modeling server (www.cbs.dtu.dk/services/CPHmodels/).^[20] The model was made on the basis of the structure of phenylacetone MO (PDB 1W4X).

The target genes were amplified by PCR by using genomic DNA of *R. jostii* RHA1 as a template, and they were subsequently cloned into pBADNS by using the In-Fusion PCR Cloning kit by following the recommendations of the manufacturer. The mutations were introduced through the QuikChange Site-Directed Mutagenesis Kit from Stratagene by following the recommendations of the manufacturer.

For expression, cells were grown in baffled flasks with lysogeny broth (LB) medium (800 mL) supplemented with ampicillin and arabinose (50 $\mu\text{g mL}^{-1}$) concentrations of 0.002% (FMO-E and FMO-G) and 0.2% (FMO-F) by shaking at 200 rpm at 24 °C for 32 h, based on the optimal expression conditions previously determined.^[6] Cell extracts were prepared by sonication with subsequent centrifugation to obtain the cleared cell extracts. Purification of the enzymes from the cleared cell extracts was done with Strep-Tactin® Sepharose from IBA GmbH by following the recommendations of the manufacturer. As a minor modification, FAD (10 μM), dithiothreitol (DTT; 1.0 mM), and 10% glycerol were added to the buffer.

Determination of kinetic parameters of FMO-E

Activities of purified FMO-E were determined spectrophotometrically by monitoring the increase or decrease in NADPH or NADH in time at 340 nm. The reaction mixture (1.0 mL) typically contained 50 mM Tris/Cl, pH 7.5 (10% glycerol, 1.0 mM DTT, 1.0 mM EDTA, 10 μ M FAD), 150 μ M coenzyme NADPH or NADH, 50 μ M ketone substrate, 5.0% dioxane, and 0.10 μ M enzyme at 25 °C. Kinetic parameters were obtained by fitting the data as previously described.^[21]

Stopped-flow experiments

The reductive and oxidative half-reactions of FMO-E were both analyzed by using an Applied Photophysics SX17 MV stopped-flow instrument equipped with a photodiode array detector. All experiments described were performed at 25 °C in 50 mM Tris/Cl (10% glycerol, 1.0 mM DTT, 1.0 mM EDTA) at pH 7.5. All concentrations stated are those in the reaction chamber after mixing. Anaerobic conditions were achieved by flushing the system and solutions with N₂ and removing trace amounts of oxygen upon addition of 1.0 mM putrescine and a catalytic amount of putrescine oxidase. The rate of reduction of FMO-E by NADPH was assessed under anaerobic conditions by adding equimolar amounts of NADPH. The reoxidation of the reduced flavin was achieved by mixing NADPH-reduced FMO-E with aerated buffer and following the spectral changes of the flavin cofactor in time. The obtained spectra were analyzed by means of numerical integration methods by using Pro-K (Applied Photophysics Ltd.), which yielded the observed rate constants.

Bioconversions with cleared cell extracts

Conversions were performed as previously described.^[6] For determining the exact concentration of each enzyme in the respective extract, a recently developed method was used that relies on the decrease in the absorbance at 450 nm upon NADPH-mediated reduction of the flavin cofactor.^[22]

Whole-cell conversions

Bioconversion of a set of 14 target compounds was performed by using cells expressing FMO-E, FMO-F, and FMO-G by employing the above-mentioned expression conditions. Cells were grown with optical density OD₅₉₀ = 0.2–0.6 at 37 °C. The cultures were then cooled to 24 °C and L-arabinose was added to the appropriate final concentration. Cyclodextrin (4.0 mM) was supplemented as a cell-membrane transfer agent. This mixture was thoroughly shaken and then divided into aliquots (1.0 mL) in a 24-well plates. Substrates were added as solutions in 1,4-dioxane (5.0 μ L, 0.8 M, 5.0 mM final concentration), and the plates were sealed with adhesive film (EasySEAL, Greiner Bio One) and incubated in an orbital shaker (Infors HT Multitron 2) at 24 °C for 24 h. Analytical samples were prepared by extraction of the biotransformation culture (0.5 mL) with EtOAc (1.0 mL, supplemented with 1.0 mM methyl benzoate as internal standard) after centrifugal separation of the cell mass (\approx 15 kRCF, 1 min, RT). All transformations were performed as technical triplicates; conversion and selectivity are reported as arithmetic mean values. Absolute configuration or optical rotation values of lactone products were assigned on the basis of published

reference biotransformations for substrates 4–9,^[14] for substrate 11,^[16] and for substrates 1 and 14–16.^[15]

Acknowledgements

This research was financially supported by the Integrated Biosynthesis Organic Synthesis (IBOS) program of the Netherlands Organisation for Scientific Research (NWO) and the European Union's Seventh Framework Programme (FP7/2007–2013) under grant agreement n°212281 (project OXYGREEN).

Keywords: Baeyer–Villiger monooxygenases · biocatalysis · cofactors · enantioselectivity · flavin-containing monooxygenases

- [1] D. E. Torres Pazmiño, M. Winkler, A. Glieder, M. W. Fraaije, *J. Biotechnol.* **2010**, *146*, 9–24.
- [2] W. J. H. van Berkel, N. M. Kamerbeek, M. W. Fraaije, *J. Biotechnol.* **2006**, *124*, 670–689.
- [3] G. de Gonzalo, M. D. Mihovilovic, M. W. Fraaije, *ChemBioChem* **2010**, *11*, 2208–2231.
- [4] D. M. Ziegler, *Trends Pharmacol. Sci.* **1990**, *11*, 321–324.
- [5] A. Rioz-Martínez, M. Kopacz, G. de Gonzalo, D. E. Torres Pazmiño, V. Gotor, M. W. Fraaije, *Org. Biomol. Chem.* **2011**, *9*, 1337.
- [6] A. Riebel, G. de Gonzalo, M. W. Fraaije, *J. Mol. Catal. B* **2013**, *88*, 20–25.
- [7] C. N. Jensen, J. Cartwright, J. Ward, S. Hart, J. P. Turkenburg, S. T. Ali, M. J. Allen, G. Grogan, *ChemBioChem* **2012**, *13*, 872–878.
- [8] M. W. Fraaije, J. Wu, D. P. H. M. Heuts, E. W. van Hellemond, J. H. L. Spelberg, D. B. Janssen, *Appl. Microbiol. Biotechnol.* **2005**, *66*, 393–400.
- [9] D. Sheng, D. P. Ballou, V. Massey, *Biochemistry* **2001**, *40*, 11156–11167.
- [10] I. A. Mirza, B. J. Yachnin, S. Wang, S. Grosse, H. Bergeron, A. Imura, H. Iwaki, Y. Hasegawa, P. C. K. Lau, A. M. Berghuis, *J. Am. Chem. Soc.* **2009**, *131*, 8848–8854.
- [11] R. Orru, H. M. Dudek, C. Martinoli, D. E. Torres Pazmiño, A. Royant, M. Weik, M. W. Fraaije, A. Mattevi, *J. Biol. Chem.* **2011**, *286*, 29284–29291.
- [12] E. Malito, A. Alfieri, M. W. Fraaije, A. Mattevi, *Proc. Natl. Acad. Sci. USA* **2004**, *101*, 13157–13162.
- [13] A. Alfieri, E. Malito, R. Orru, M. W. Fraaije, A. Mattevi, *Proc. Natl. Acad. Sci. USA* **2008**, *105*, 6572–6577.
- [14] F. Rudroff, J. Ryzd, F. H. Ogink, M. Fink, M. D. Mihovilovic, *Adv. Synth. Catal.* **2007**, *349*, 1436–1444.
- [15] M. D. Mihovilovic, P. Kapitán, P. Kapitánová, *ChemSusChem* **2008**, *1*, 143–148.
- [16] M. J. Fink, D. V. Rial, P. Kapitánová, A. Lengár, J. Rehdorf, Q. Cheng, F. Rudroff, M. D. Mihovilovic, *Adv. Synth. Catal.* **2012**, *354*, 3491–3500.
- [17] H. M. Dudek, D. E. Torres Pazmiño, C. Rodríguez, G. Gonzalo, V. Gotor, M. W. Fraaije, *Appl. Microbiol. Biotechnol.* **2010**, *88*, 1135–1143.
- [18] N. M. Kamerbeek, M. W. Fraaije, D. B. Janssen, *Eur. J. Biochem.* **2004**, *271*, 2107–2116.
- [19] J. D. Thompson, D. G. Higgins, T. J. Gibson, *Nucleic Acids Res.* **1994**, *22*, 4673–4680.
- [20] M. Nielsen, C. Lundegaard, O. Lund, T. N. Petersen, *Nucleic Acids Res.* **2010**, *38*, W576–81.
- [21] D. E. Torres Pazmiño, R. Snajdrova, B.-J. Baas, M. Ghobrial, M. D. Mihovilovic, M. W. Fraaije, *Angew. Chem.* **2008**, *120*, 2307–2310; *Angew. Chem. Int. Ed.* **2008**, *47*, 2275–2278.
- [22] A. Riebel, H. M. Dudek, G. Gonzalo, P. Stepniak, L. Rychlewski, M. W. Fraaije, *Appl. Microbiol. Biotechnol.* **2012**, *95*, 1479–1489.

Received: July 10, 2013

Revised: August 19, 2013

Published online on October 7, 2013